

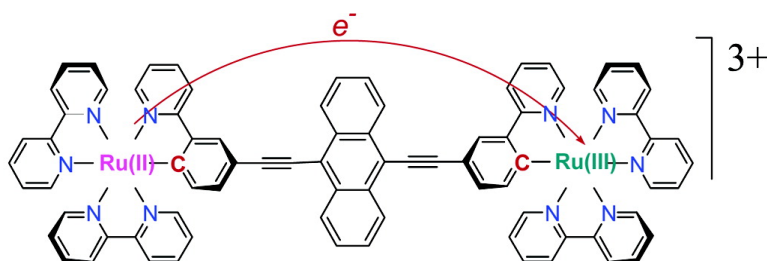
Article

Molecular Wires Built from Binuclear Cyclometalated Complexes

Sandrine Fraysse, Christophe Coudret, and Jean-Pierre Launay

J. Am. Chem. Soc., **2003**, 125 (19), 5880-5888 • DOI: 10.1021/ja0299506 • Publication Date (Web): 18 April 2003

Downloaded from <http://pubs.acs.org> on March 26, 2009



More About This Article

Additional resources and features associated with this article are available within the HTML version:

- Supporting Information
- Links to the 18 articles that cite this article, as of the time of this article download
- Access to high resolution figures
- Links to articles and content related to this article
- Copyright permission to reproduce figures and/or text from this article

[View the Full Text HTML](#)

Molecular Wires Built from Binuclear Cyclometalated Complexes

Sandrine Fraysse, Christophe Coudret,* and Jean-Pierre Launay*

Contribution from the CEMES-CNRS, 29, Rue Jeanne Marvig, BP 4347,
31055 Toulouse Cedex 4, France

Received December 28, 2002; E-mail: coudret@cemes.fr; launay@cemes.fr

Abstract: Binuclear complexes with cyclometalated ends of the $[\text{Ru}(\text{bpy})_2(\text{ppH})]^+$ type (bpy = 2,2'-bipyridine, ppH = 2-phenylpyridine), linked by various spacers, have been prepared. These spacers are made of one or two triple bonds, or bis-ethynyl aryl groups, with aryl = benzene, thiophene, or anthracene. The complexes with bis-ethynyl aryl spacers are obtained by Sonogashira couplings with suitable bis-alkynes, starting from the $[\text{Ru}(\text{bpy})_2(\text{ppBr})]^+$ synthon. Complexes with one or two triple bonds are obtained from the true alkyne $[\text{Ru}(\text{bpy})_2(\text{pp-CCH})]^+$ cyclometalated precursor, using respectively a Sonogashira coupling with the iodo derivative $[\text{Ru}(\text{bpy})_2(\text{ppI})]^+$, or an oxidative homocoupling. Some complexes with *tert*-butyl-substituted bipyridine ancillary ligands have also been obtained. Oxidation of the binuclear complexes occurs near 0.5 V, i.e., more easily than with $[\text{Ru}(\text{bpy})_3]^{2+}$ -based complexes. A single anodic wave is observed, with almost no detectable splitting, corresponding to two closely spaced one-electron processes. Differential pulse voltammetry allows the determination of the corresponding comproportionation constants involving the mixed valence $\text{Ru}^{\text{II}}-\text{Ru}^{\text{III}}$ forms. Controlled potential electrolysis yields the mixed valence forms in comproportionation equilibrium with homovalent forms. Analysis of the intervalence transitions allows the calculation of the electronic coupling element V_{ab} . This series of complexes exhibit relatively large couplings when comparing with complexes of similar metal-metal distances, with a special mention for the anthracene-containing spacer, which appears particularly efficient for mediating the metal-metal interaction. The results can be rationalized by theoretical calculations at the extended Hückel level.

Introduction

The study of intramolecular electron transfer through mixed-valence compounds is a very active field of research. A large number of compounds have been synthesized, allowing the study of various factors such as distance, solvent effect, and bridge nature.¹ From a practical point of view, the electron transfer process is probed by the intensity of the intervalence transition (IT), according to the relation devised by N. Hush 35 years ago.² This yields the electronic coupling parameter V_{ab} describing the amount of electronic interaction between remote sites. From this interaction, one can devise general rules for the design of efficient bridging ligands allowing long-distance electron transfer. In addition, mixed-valence compounds can be simple models for the expanding domain of nanojunctions, in which a single molecule is bridging two nanoscale metallic conductors. For such systems, experimental and theoretical results begin to be available.³

However, as the size of the compounds increase, synthetic problems become more acute, with in particular a decrease in free ligand solubility. In addition, the electronic coupling decreases and its detection becomes problematic. Thus there is a need for new classes of compounds that would be more easily accessible and would exhibit stronger metal-metal couplings than conventional systems.

Cyclometalated complexes offer attractive characteristics. The existence of the ruthenium-carbon bond increases markedly the electronic coupling with respect to compounds containing only ruthenium-nitrogen bonds,⁴ so that the synthesis of bis-cyclometalated complexes is of strategic interest. In the past decade, a new approach for the synthesis of this type of dinuclear complexes has emerged, based on the use of suitably activated monomeric complexes as classic organic synthons for palladium-catalyzed carbon-carbon coupling reactions, thus obviating solubility or fragility problems of the conjugated bridging ligand. In most of the cases, it implies the preparation of specifically halogenated or boronated ligands, such as in the case of

(1) Some reviews on intramolecular electron transfer in mixed-valence systems: (a) Creutz, C. *Prog. Inorg. Chem.* **1983**, *30*, 1. (b) Crutchley, R. *J. Adv. Inorg. Chem.* **1994**, *41*, 273. (c) Brunschwig, B. S.; Sutin, N. *Coord. Chem. Rev.* **1999**, *187*, 233. (d) Kaim, W.; Klein, A.; Glöckle, M. *Acc. Chem. Res.* **2000**, *33*, 755. (e) Nelsen, S. F. In *Electron Transfer in Chemistry*; Balzani, V., Ed.; Wiley-VCH: Weinheim, Germany, 2001; Vol. 1, Chapter 10. (f) Launay, J.-P.; Coudret, C. In *Electron Transfer in Chemistry*; Balzani, V., Ed.; Wiley-VCH: Weinheim, Germany, 2001; Vol. 5, Chapter 1. (g) Launay, J.-P. *Chem. Soc. Rev.* **2001**, *30*, 386-397. (h) Demadis, K. D.; Hartshorn, C. M.; Meyer, T. J. *Chem. Rev.* **2001**, *101*, 2655. (i) Brunschwig, B. S.; Creutz, C.; Sutin, N. *Chem. Soc. Rev.* **2002**, *31*, 168.

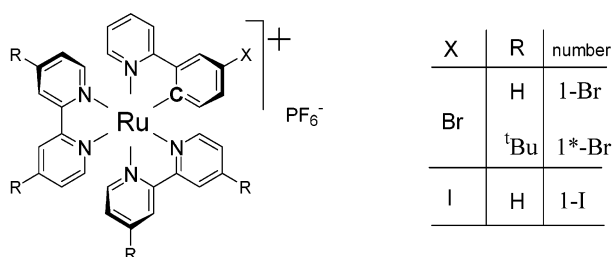
(2) Hush, N. S. *Prog. Inorg. Chem.* **1967**, *8*, 391.

(3) Reed, M. A.; Zhou, C.; Muller, C. J.; Burgin, T. P.; Tour, J. M. *Science* **1997**, *278*, 252. Tans, S. J.; Devoret, M. H.; Dai, H.; Thess, A.; Smalley, R. E.; Geerlings, L. J.; Dekker, C. *Nature* **1997**, *386*, 474. Kergueris, C.; Bourgoin, J.-P.; Palacin, S.; Esteve, D.; Urbina, C.; Magoga, M.; Joachim, C. *Phys. Rev. B* **1999**, *59*, 12505. Magoga, M.; Joachim, C. *Phys. Rev. B* **1997**, *56*, 4722.

(4) (a) Beley, M.; Collin, J.-P.; Sauvage, J.-P. *Inorg. Chem.* **1993**, *32*, 4539-4543. (b) Patoux, C.; Launay, J.-P.; Beley, M.; Chodorowski-Kimmes, S.; Collin, J.-P.; James, S.; Sauvage, J.-P. *J. Am. Chem. Soc.* **1998**, *120*, 3717-3725.

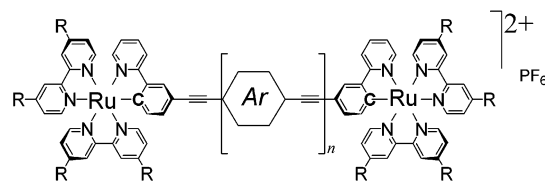
ruthenium poly-imine complexes⁵ or cyclometalated ruthenium complexes derived from the 1,3-dipyridylbenzene ligand.⁶ A major improvement of this synthesis is achieved when the ligand can be functionalized *after* the complexation step, as known for 1,3-diketone derivatives.⁷

Following these lines, some years ago, we have reported that the complex $[\text{Ru}(\text{bpy})_2(\text{ppH})]^+$ (ppH = 2-phenylpyridine) undergoes a regioselective halogenation yielding complexes **1-Br** and **1-I** on the phenyl ring, at the *para* position to the ruthenium-carbon bond.⁸ These bromo- and iodo complexes have been shown to be suitable synthons⁹ for palladium-catalyzed reactions, thanks to their solubilities in polar or halogenated solvents and to their ease of purification via conventional chromatographic techniques. Hence our approach was to exploit these remarkable synthetic potentialities, thus avoiding the preparation of a specifically substituted phenylpyridine.



The $[\text{Ru}(\text{bpy})_2(\text{ppX})]^+$ organometallic synthon is particularly well suited for cross-coupling reactions (e.g., of the Sonogashira type) with alkynes, thus allowing the construction of long binuclear complexes in which the bridge contains spacers of the tolane type (Figure 1), i.e., an alternation of triple bonds and aromatic moieties. Such rigid and conjugated spacers are currently used in a number of studies of intramolecular electron and energy transfer processes.¹⁰

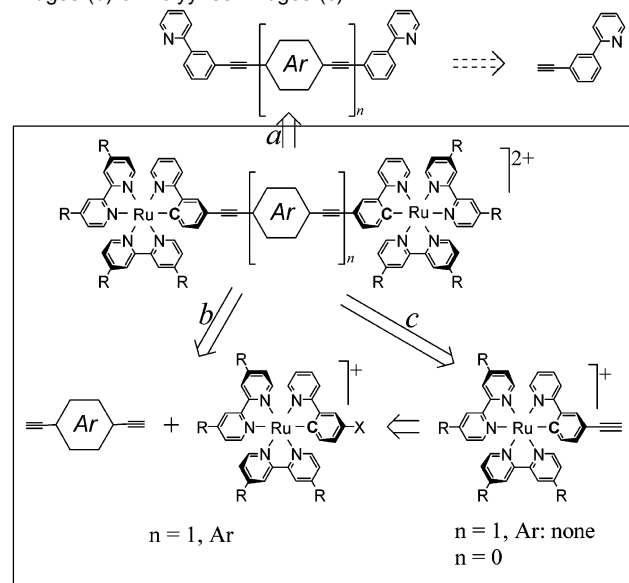
Finally, the $[\text{Ru}(\text{bpy})_2(\text{ppX})]^+$ fragment offers an additional synthetic flexibility by proper substitution on the ancillary bipyridine ligands. The introduction of donor or acceptor groups *para* to nitrogen modulates the electron density on the metal as shown by changes in its redox potential. This can be considered as a way of fine-tuning the energy levels of the redox groups with respect to those of the central spacer. In the present paper, we have considered only the case of donor substituents, using 4,4'-di-*tert*-butyl-2,2'-bipyridine (bpy*). A preliminary report dealing with complexes with normal bipyridine as ancillary ligands has been published elsewhere.⁹



<i>n</i>	Ar	R	compound number
1		H	2
		^t Bu	2*
		H	3
		^t Bu	3*
		H	4
0	none	H	5
	—	H	7

Figure 1. Classification of compounds of the present paper.

Scheme 1. Retrosynthetic Route: (a) Conventional Synthesis; (Box) Building Block Strategies for Oligoethynylene-Arenylene Bridges (b) or Polyynes Bridges (c)



Results and Discussion

Syntheses. Our first strategy was to react the organometallic building block **1-Br** with various diethynylarenes under the palladium/copper-catalyzed aromatic ethynylation methodology.¹⁰

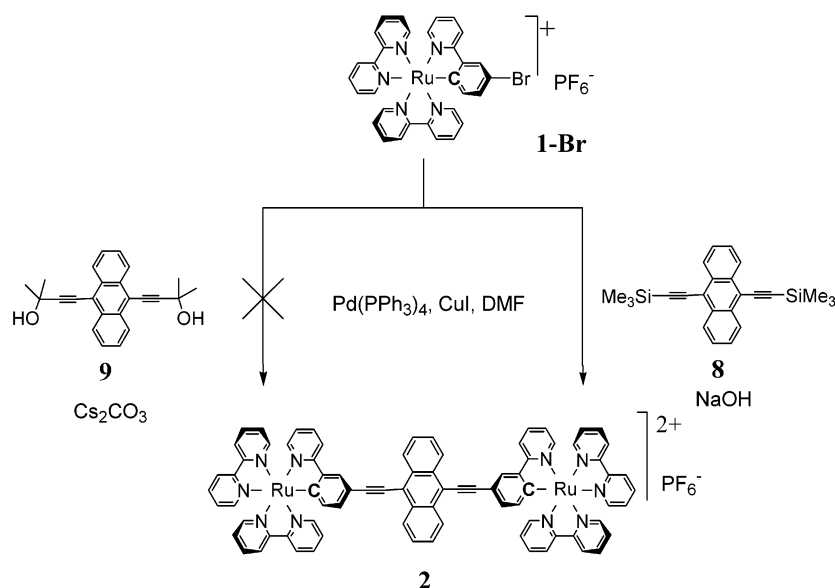
9,10-Diethynylantracene is readily available from two protected forms: the bis-TMS **8**¹¹ or the bis-dimethylcarbinol **9**.¹² Submitted to classic Sonogashira conditions ($\text{Pd}(\text{PPh}_3)_4$, CuI,

- (5) Connors, P. J., Jr.; Tzalis, D.; Dunnick, A. L.; Tor, Y. *Inorg. Chem.* **1998**, *37*, 1121–1123. Tzalis, D.; Tor, Y. *J. Am. Chem. Soc.* **1997**, *118*, 8852–8853. Tzalis, D.; Tor, Y. *Chem. Commun.* **1996**, 1043–1044. Hissler, M.; El-Ghayouri, A.; Harriman, A.; Ziessel, R. *Angew. Chem., Int. Ed.* **1998**, *37*, 1717–1720. Dunne, S. J.; Constable, E. C. *Inorg. Chem. Commun.* **1998**, *1*, 167–169. Aspley, C. J.; Williams, J. A. G. *New J. Chem.* **2001**, *25*, 1136–1147. Tor, Y. *Synlett* **2002**, 1043–1054.
- (6) Chodorowsky-Kimmes, S.; Beley, M.; Collin, J.-P.; Sauvage, J.-P. *Tetrahedron Lett.* **1996**, *37*, 2963–2966.
- (7) Kasahara, Y.; Hoshino, Y.; Kajitani, M.; Shimizu, K.; Sato, G. P. *Organometallics* **1992**, *11*, 1968–1971. Hoshino, Y.; Suzuki, T.; Umeda, H. *Inorg. Chim. Acta* **1996**, *245*, 87–90.
- (8) Coudret, C.; Fraysse, S.; Launay, J.-P. *J. Chem. Soc., Chem. Comm.* **1998**, 663–664.
- (9) Fraysse, S.; Coudret, C.; Launay, J.-P. *Tetrahedron Lett.* **1998**, *39*, 7873–7876.
- (10) Sonogashira, K.; Tohda, Y.; Hagihara, N. *Tetrahedron Lett.* **1975**, *50*, 4467–4470. Ziessel, R.; Suffert, J.; Youinou, M.-T. *J. Org. Chem.* **1996**, *61*, 6535–6546. El-Ghayoury, A.; Harriman, A.; Ziessel, R. *J. Phys. Chem. A* **2000**, *104*, 7906–7915.

(11) Kobayashi, E.; Jiang, J.; Furukawa, J. *Polym. J.* **1990**, *22*, 266–273.

(12) Adapted from ref 13 using a 2:1 THF/DIPA mixture. For the use of THF as cosolvent, see: Thorand, S.; Krause, N. *J. Org. Chem.* **1998**, *63*, 8551–8553.

Scheme 2. Synthesis of the Binuclear Complex 2



$i\text{Pr}_2\text{NH}$, DMF, 80 °C) with the complex **1-Br**, the coupling was found to be very sluggish and gave a complex mixture from which a low yield of an impure sample of dinuclear complex was obtained. This was attributed to the poor reactivity of the complex **1-Br** as already mentioned⁸ and also to the relative instability of the unprotected 9,10-diethynylanthracene especially in this reaction medium. For this reaction, it is admitted that the amine is used as a base to generate a cuprous acetylide, which would then transfer an alkynyl ligand to an arylpalladium species.¹⁴ Since a base is also needed to cleave the protective group of the alkyne precursor, we thought that combining these two reactions would allow us to achieve a slow release of the unstable ethynylarene. There are few reports in which the amine is deliberately replaced by an inorganic base such as K_2CO_3 ,¹⁵ showing that the reaction still takes place under such heterogeneous conditions. Some examples can be found where an unstable alkyne is deprotected in the presence of appropriate reagents to undergo an oxidative dimerization or an arylation. This strategy has been mostly developed for carbinol-protected alkynes, the deprotection of which usually requires forcing conditions:¹³ it involves hydroxide bases with phase transfer conditions.¹⁶ In our case, replacing the diisopropylamine by Cs_2CO_3 and using **9** as alkyne source gave no reaction, even after prolonged heating (16 h at 110 °C). The use of a stronger base, potassium hydroxide, gave only partially coupled mononuclear complex. Eventually, we thought of using the bis-TMS **8** as well as sodium hydroxide as reagents. In situ desilylation by methanolic K_2CO_3 for Eglinton oxidative coupling was known,¹⁷ but no such reagents were reported for Sonogashira ethynylation.¹⁸

This approach was found to be fruitful since the heating of a DMF solution of all the reagents to 80 °C in the presence of

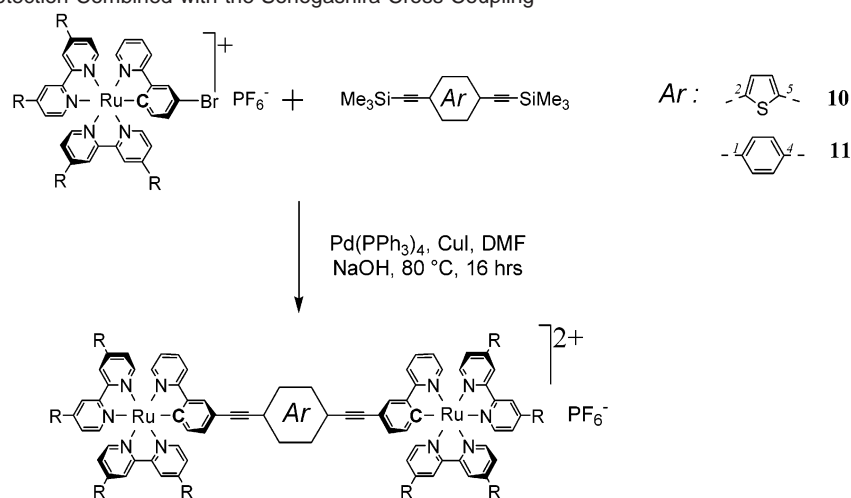
solid potassium hydroxide for 16 h afforded the dinuclear complex **2** in 34% yield after purification on a preparative TLC plate. This rather surprising result, since the hydroxide ions should rapidly cleave the TMS group, may be explained by the low solubility of solid sodium hydroxide in the reaction mixture (the pellet is found almost unchanged once the reaction is quenched) and by a possible role of phase transfer agent played by the cationic ruthenium complex. (Under similar conditions, cuprous halide *alone* may also promote alkyne desilylation.¹⁹) These reaction conditions were then extended to the thiophene (**10**) and the benzene (**11**) derivative. Yields of these “one-pot” coupling remain moderate with sensitive alkynes such as **10**, and markedly better with the more stable 1,4-diethynylbenzene derivative **11**. Note that the use of the more reactive iodo derivative **1-I** gave an unexpected scrambled arylphosphine oxide.²⁰

To tune the redox potential of the Ru(II)/Ru(III) couple by modification of the ancillary ligand, we have also used **1-Br*** as starting organometallic synthon, i.e., a compound in which the usual 2,2'-bipyridine is replaced by 4,4'-di-*tert*-butyl-2,2'-bipyridine. Using the same one-pot in situ deprotection/cross-coupling technique with **8** and **10**, the compounds **2*** and **3*** are obtained. The yield is, however, poor (20 and 25%, respectively) because the obtained complexes are very soluble in most organic solvents and thus difficult to purify.

Dinuclear complexes **5** and **7**, bridged respectively by two or one triple bond, required the use of the complex bearing a terminal alkyne. Once again we have applied a one-pot deprotection–homocoupling protocol. Indeed, heating a solution of complex **12** in the presence of CuI and KOH in air for 15 h provides the homocoupled complex, albeit in rather poor yield. No effort were made to improve this route.

(13) MacBride, J. A. H.; Wade, K. *Synth. Commun.* **1996**, *26*, 2309–2316.
 (14) Sonogashira, K. In *Metal-Catalyzed Cross-Coupling Reactions*; Diederich, F., Stang, P. J., Eds.; Wiley-VCH: Weinheim, Germany, 1998; pp 203–229.
 (15) Eckert, T.; Ipaktschi, J. *Synth. Commun.* **1998**, *28*, 327–335.
 (16) Carpita, A.; Lessi, A.; Rossi, R. *Synthesis* **1984**, 571–572. Huynh, C.; Linstrumelle, G. *Tetrahedron* **1988**, *44*, 6337–6344. Nye, S. A.; Potts, K. T. *Synthesis* **1988**, 375–377. Solomin, V. A.; Heitz, W. *Macromol. Chem. Phys.* **1994**, *195*, 303–314. Godinez, C. E.; Zepeda, G.; Garcia-Garibay, M.-A. *J. Am. Chem. Soc.* **2002**, *124*, 4701–4707.

(17) Haley, M. M.; Bell, M. L.; Brand, S. C.; Kimball, D. B.; Pak, J. J.; Wan, W. B. *Tetrahedron Lett.* **1997**, *38*, 7483–7486.
 (18) A similar approach was disclosed at almost the same time as ours, with methanolic K_2CO_3 as base: Schultz, D. A.; Gwaltney, K. P.; Lee, H. J. *Org. Chem.* **1998**, *63*, 4034–4038. For aqueous KOH see: Pak, J. J.; Weakley, T. J. R.; Haley, M. M. *J. Am. Chem. Soc.* **1999**, *121*, 8182–8192.
 (19) Nishihara, Y.; Ikegasaki, K.; Hirabayashi, K.; Ando, J.; Mori, A.; Hiyama, T. *J. Org. Chem.* **2000**, *65*, 1780–1787.
 (20) Frayse, S.; Coudret, C. *Tetrahedron Lett.* **1999**, *40*, 9249.

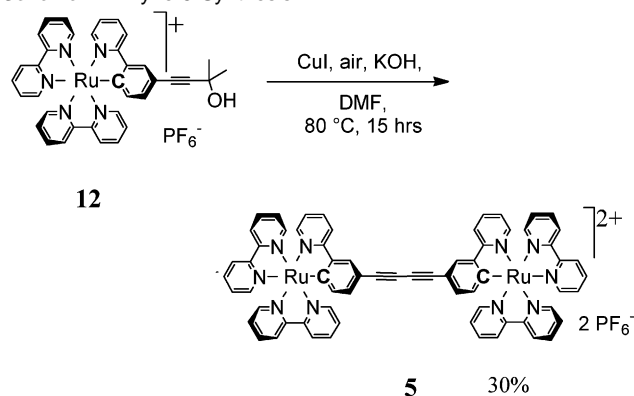
Scheme 3. In Situ Deprotection Combined with the Sonogashira Cross-Coupling

	R	number	yield
	H	2	34%
	^t Bu	2*	20%
	H	3	39%
	^t Bu	3*	25%
	H	4	60%

To obtain **7**, we considered a route involving a Sonogashira coupling with the terminal alkyne **13**, and thus a preparation of the latter was necessary. The moderate yield of the previous one-pot deprotection/oxidative coupling was attributed to an inefficient unmasking of the terminal alkyne. As we reported previously, the use of a stronger base than the carbinol to be cleaved, namely, potassium *tert*-butoxide in refluxing THF, resulted in the total conversion of the starting material within 2 h and crude material could be used without any purification other than the elimination of salts and ion-exchange.²¹

Next, the cross-coupling was attempted first with the bromo complex **1-Br**. As previously noted, the reaction was found to be sluggish, and, despite drastic precautions against oxidation, the desired product **7** was always contaminated by the homo-coupled complex **5**, their separation being impossible due to the similarity of their structures and charges. To perform the reaction at a lower temperature, we then used the iodo complex **1-I**, for which the coupling was achieved with a 40% isolated yield.

To obtain a binuclear complex with a long metal–metal separation, the association of several aryl groups is necessary. From our previous results it was clear that due to the poor reactivity of the bromide **1-Br**, our route had to start from the terminal alkyne **13**. Thus a highly convergent strategy was designed, starting from the 2-iodo-5-trimethylsilylethynylthiophene **14**, easily available in two steps from 2-iodothiophene by a TMSA ethynylation followed by a lithiation–iodination

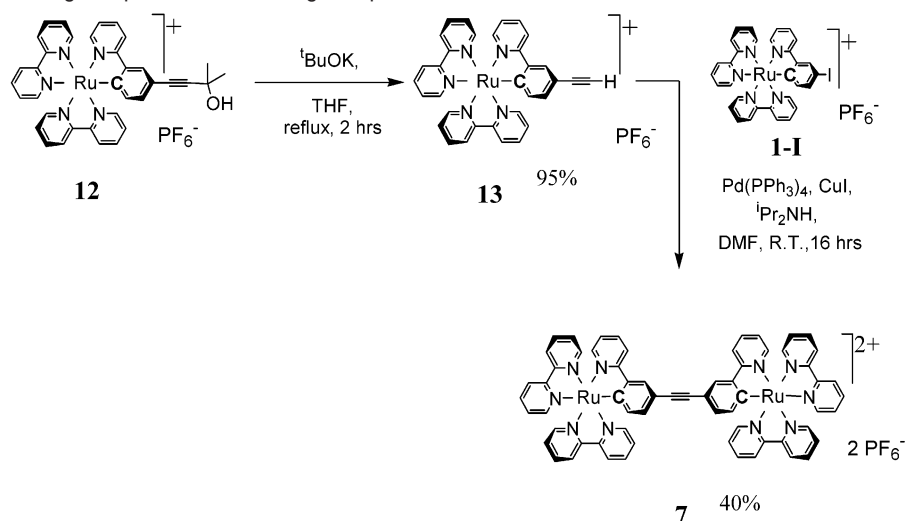
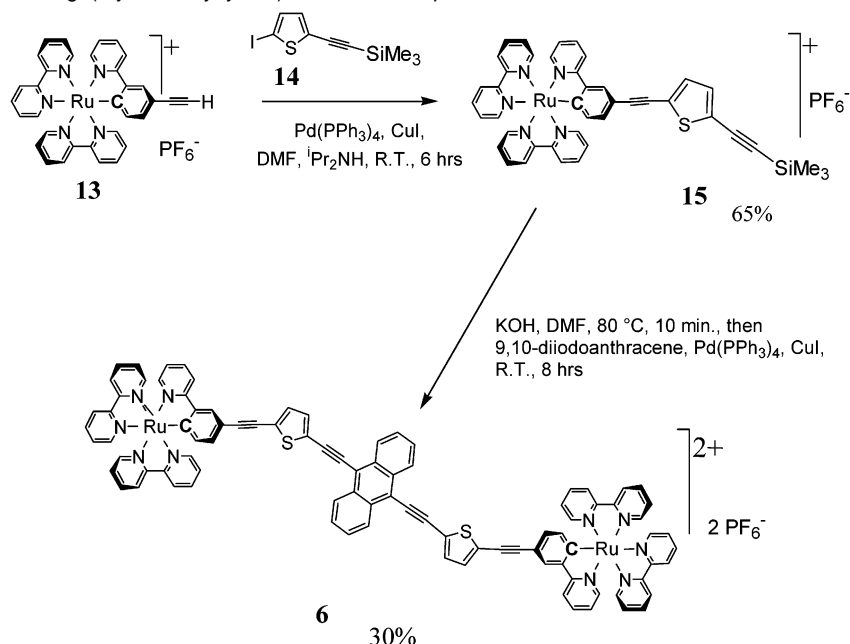
Scheme 4. Diyne 5 Synthesis

step.²² This aryl iodide was found to react remarkably efficiently at room temperature with the organometallic alkyne **13** since the mononuclear complex **15** was isolated with a 65% yield. Eventually, a deprotection of **15** by aqueous potassium hydroxide followed by a coupling with 9,10-diiodoanthracene afforded **6**, for which the metal–metal distance reaches 32.8 Å according to molecular modeling.

General Properties. All complexes have been fully characterized by NMR. The organometallic [Ru(bpy)₂(pp)] moieties can exhibit either Δ or Λ chirality, so that mixtures of stereoisomers are actually obtained. However, the protons of the chiral centers are far enough to be two-by-two equivalent, and no splitting of NMR signals was observed.

(21) Fraysse, S.; Coudret, C.; Launay, J.-P. *Eur. J. Inorg. Chem.* **2000**, 1581–1590.

(22) Viola, E.; Lo Sterzo, C.; Trezzi, F. *Organometallics* **1996**, *15*, 4352–4354.

Scheme 5. Route to the Single Triple Bond Containing Complex **7****Scheme 6.** Synthesis of the Oligo(arylene-ethynylene) Dinuclear Complex **6****Table 1.** Redox Potentials and Comproportionation Constants for Binuclear Compounds (values recorded in acetonitrile containing 0.1 M NBu₄PF₆)

complex	E_1° (mV)	E_2° (mV)	K_c
4	479	547	14
2	487	544	9
3	485	542	9
5	450	579	22
7	453	551	45
6	498	541	5
2*	402	469	14
3*	482	565	26

The binuclear complexes exhibited generally a single anodic wave corresponding to the oxidation of the two metal centers, since the metal–metal distance was too long for the appearance of well-resolved waves (see Table 1). Only for compound **7** could the onset of a wave splitting be detected. The unique anodic wave occurred near 0.5 V for most complexes. Anodic and cathodic peak potentials were found independent

of the sweep rate, hence showing the Nernstian nature of the redox processes. Some cathodic shift occurred when replacing bipyridine by the more strongly donating 4,4'-di-*tert*-butyl-2,2'-bipyridine ancillary ligand, as could be anticipated.

Even when no wave splitting is observed, the electrode process is actually a succession of two very close one-electron exchanges. Since the processes are Nernstian, differential pulse voltammetry allows the precise determination of the difference in redox potentials, and hence of the comproportionation constant.²³ The obtained values (see Table 1) range between 9 and 25 (as usual for complexes of similar length),²⁴ with values outside this range for the very long compound, **6** ($K_c = 5$), and the shortest, **7** ($K_c = 45$).

(23) Richardson, D. E.; Taube, H. *Inorg. Chem.* **1981**, *20*, 1278–1285.(24) Ribou, A.-C.; Launay, J.-P.; Takahashi, K.; Nihira, T.; Tarutani, S.; Spangler, C. W. *Inorg. Chem.* **1994**, *33*, 1325–1329. Ribou, A.-C.; Launay, J.-P.; Sachtleben, M.; Li, H.; Spangler, C. W. *Inorg. Chem.* **1996**, *35*, 3735–3740.

Table 2. UV–Vis Spectra of 4, 2, 3, 5, 6, and 7 in Acetonitrile

complex	λ_{max} , nm ($10^{-4} \epsilon$, mol $^{-1}$ L cm $^{-1}$)
4	249 (7.60), 298 (15.7), 397 (5.80), 477 (2.88), 550 (sh)
2	261 (10.9), 297 (16.0), 360 (3.81), 416 (3.00), 535 (6.68)
3	249 (10.9), 297 (15.9), 360 (sh), 408 (6.37), 468 (4.52), 550 (sh)
5	248 (18.9), 296 (32.0), 374 (11.8), 400 (sh), 482 (6.50), 550 (sh)
6	250 (17.0), 365 (5.0), 500 (5.8)
7	250 (10.2), 285 (16.1), 365 (3.37), 400 (sh), 483 (1.68), 550 (sh)

UV–visible spectra are given in Table 2. They exhibit rich and complex spectra with an intense sharp band near 300 nm and several less intense bands in the 350–600 nm range.

Although a detailed assignment is presently out of reach, the 350–600 nm bands seem to be due to metal-to-bipyridine charge transfer transitions.²⁵ Bipyridine is indeed the best acceptor in the coordination sphere of ruthenium. Since the substituted phenylpyridine ligands are donor ligands, they make ruthenium more electron rich than in conventional Ru-trisbipyridine complexes. This would explain that the charge transfer transitions occur here at a lower energy than in [Ru(bpy)₃]²⁺ and its substituted variants. The most spectacular change in the present series is the particularly high intensity of the lowest energy band (535 nm, $\epsilon = 66\,800$) in the case of the anthracene-containing dimer **2**. No obvious explanation was found for this effect, except that this intensity enhancement could be due to more delocalization either in the ground or in the excited state.

Intervalence Transitions and Electronic Couplings. After determination of the comproportionation equilibrium constants K_c by differential pulse voltammetry, each compound was subject to a controlled potential electrolysis to generate the mixed valence species (see Experimental Section). The oxidized species were found stable, and the quantities of electricity necessary for the complete oxidation agreed with the theoretical values within 10%. During oxidation, a ligand-to-metal-charge transfer (LMCT) band appeared near 800–900 nm and reached its maximum intensity for the complete oxidation to Ru(III)–Ru(III). The intervalence bands appeared as weak shoulders or extra absorption on the long-wavelength side, and their intensity culminated at half-oxidation. A deconvolution of the spectra was performed in all cases. Compounds with one or two triple bonds (**7** and **5**, respectively) gave intervalence transitions at lower energies than the others, so that they were better resolved (Figure 2), a fact attributed to their shorter length.

Experimental results on the intervalence transitions (position, extinction coefficient, width) are gathered in Table 3. Disappointingly, the longest compound, **6**, did not exhibit a measurable intervalence transition. The energy of the transition increases slightly with R_{MM} (i.e., the max absorption decreases, from about 1500–1800 nm for the shorter compounds **5** and **7**, to 1200–1500 nm for the longer ones **2**, **3**, **4**). This is expected from the standard model of the solvent reorganization energy.¹ Bandwidths were compared with the theoretical values coming from Hush's expression^{1a} $\Delta\nu_{1/2} = (2310\nu_{\text{max}})^{1/2}$. Experimental values were of the same order of magnitude, except for **4** (slightly narrower) and **5**, **7**, and **3***, for which they were wider by about 30%. No obvious explanation has been found for this difference. However, it should be mentioned that a large bandwidth can occur from a number of causes, among which intra- t_{2g} splitting due to the low local symmetry,^{1f} so that the

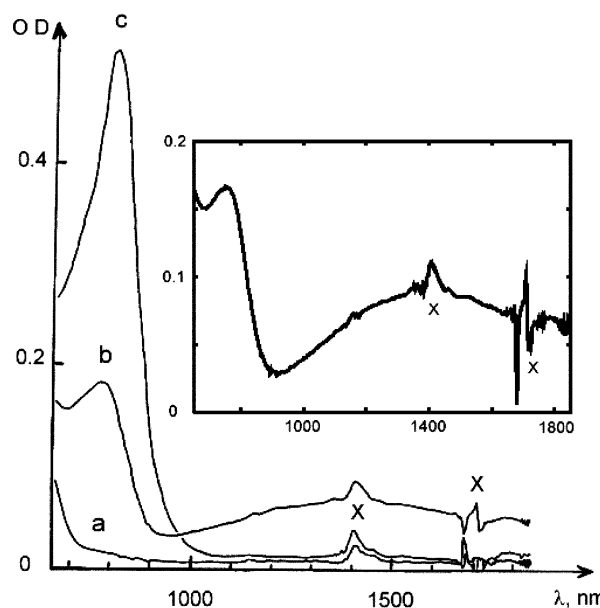


Figure 2. Example of intervalence transition, compound **5** in acetonitrile: (a) initial spectrum, (b) at half-oxidation, (c) at full oxidation. Inset: spectrum of the mixed valence form, corrected from comproportionation. \times : artifacts due to a nonperfect compensation of solvent absorption.

Table 3. Intervalence Transitions and Experimental and Theoretical V_{ab} Values for Binuclear Compounds

complex	λ_{max}^a	ϵ_{max}^b	$\Delta\nu_{1/2}(\text{exp})^c$	$\Delta\nu_{1/2}(\text{theo})^d$	R_{MM}^e	$V_{\text{ab}}(\text{exp})^f$	$V_{\text{ab}}(\text{theo})^g$
4	1200	2350	3630	4390	20.6	0.033	0.052
2	1430	6840	4150	4020	20.7	0.055	0.065
3	1300	2430	3920	4210	20.1	0.034	0.060
5	1500	2490	5170	3920	16.4	0.045	0.063
7	1800	5790	4680	3580	13.7	0.070	0.075
2*	1580	2130	3500	3820	20.7	0.027	0.063
3*	1400	1200	5000	4060	20.1	0.026	0.058

^a Band position in nm. ^b Extinction coefficient, in mol $^{-1}$ L cm $^{-1}$. ^c Full width at half-height, in cm $^{-1}$ (experimental). ^d Full width, cm $^{-1}$, computed from Hush's equation $\Delta\nu_{1/2} = (2310\nu_{\text{max}})^{1/2}$. ^e Metal–metal distance, Å. ^f Experimental V_{ab} couplings, eV. ^g Theoretical V_{ab} coupling from extended Hückel calculations.

intervalence transition can be an envelope of several overlapping bands. Thus, in the evaluation of the experimental V_{ab} coupling, we have used the experimental bandwidth, which encompasses all sub-bands.

Theoretical values of the couplings obtained by the extended Hückel method are also gathered in Table 3. We have shown elsewhere^{4b} that this method directly provides realistic values of the couplings, provided that a reasonable guess is made for the Ru(4d) energies. In the present case, we first used H_{ii} of Ru(4d) at -12 eV as justified before.^{4b} However this led to an unrealistic disposition of molecular orbitals in the Ru^{II}–Ru^{II} dimers, with for instance the HOMO of **2** being essentially anthracene-centered, while all experimental evidence shows that the metal is oxidized first. Thus we chose a slightly higher value (-11.5 eV), which results in the correct order of orbitals. Then, the theoretical values are similar to the experimental ones, and in particular they evolve in the same way when going from one compound to the other. Note that all calculations were performed with a planar disposition of the aromatic cycles connected by a triple bond.²⁶

The general trend is as follows: starting from the compound with one triple bond (**7**), the addition of a second triple bond (compound **5**) decreases the coupling. The intercalation of a

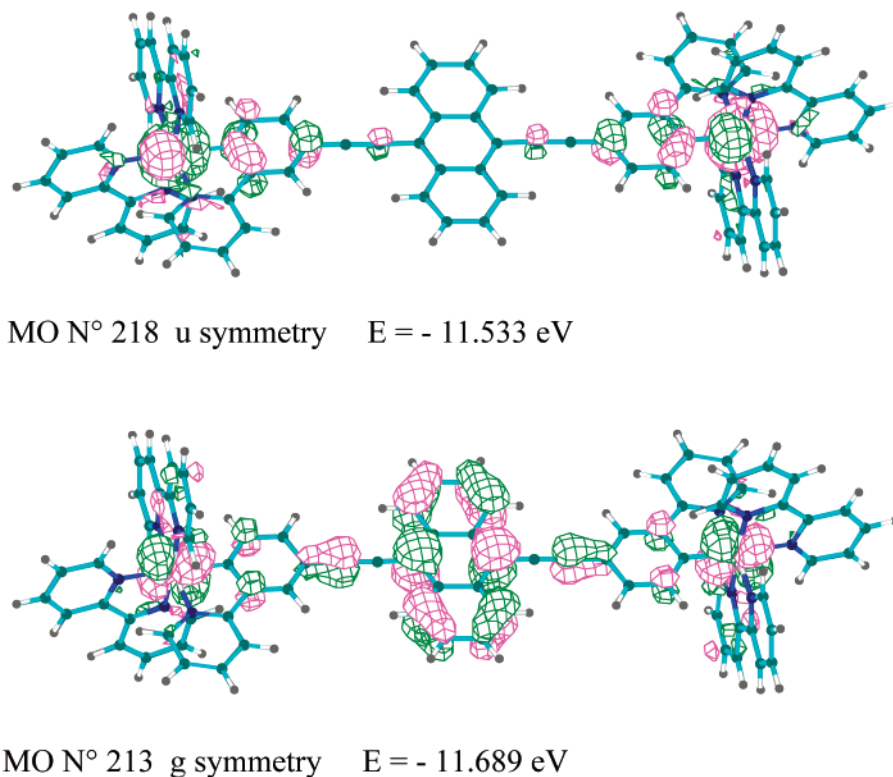


Figure 3. Molecular orbitals defining the coupling in the anthracene-containing complex **2**.

phenylene group between the triple bonds (compound **4**) decreases again the coupling, as could be anticipated. However the replacement of phenylene by anthracenylene (compound **2**) increases markedly the coupling, which becomes comparable or even slightly greater than the one for **5**, i.e., when the two triple bonds are directly linked. This trend is reproduced correctly by the calculation. Thus there is a special and particularly efficient role of the anthracenylene group for mediating the electronic interaction, while thiophene for example does not change the coupling (compound **3** gives the same V_{ab} as **4**). A similar effect has been reported by Anderson et al. with dimers of porphyrins linked by a 9,10-diethynylanthracene spacer.²⁷ The electronic communication, measured by the red shift of luminescence, is higher than for a shorter dimer *without* the anthracene part. Another observation, closer to our case, is reported by Nelsen et al.:²⁸ in organic mixed-valence compounds with hydrazine end groups, the anthracene bridge is more efficient than the benzene one, and this is also related to the better ability of anthracene to give a radical cation.

In molecular orbital terms, the explanation is straightforward: replacing the central phenylene for anthracenylene raises the HOMO of the bridge, as shown by comparative extended Hückel calculations on simplified versions of the bridge, diethynyl-

phenylbenzene (HOMO = -11.93 eV) and diethynylphenyl-anthracene (HOMO = -11.44 eV). Since the ruthenium d orbitals are expected to lie slightly above the anthracene bridge orbitals, the mixing is more efficient with the anthracene bridge. This is shown in Figure 3, where one of the orbitals defining the coupling appears much more delocalized on the anthracene part than the other. This increases the splitting between these two orbitals and, thus, by definition, the V_{ab} coupling. Figure 3 thus makes clear the role of the LMCT state in enhancing the Ru–Ru interaction.

The peculiar role of anthracene in mediating electronic effects is frequently justified in a qualitative way by the possibility of a mesomeric structure with quinoidal and cumulenyl character.^{27,29} It appears desirable to link these justifications with *bona fide* quantum chemical calculations using molecular orbitals. Such an approach is presently in progress.³⁰

For the complexes with *tert*-butyl-substituted bipyridines (**2*** and **3***), the coupling is smaller than with normal bipyridines. This appears logical, since the more strongly donating *tert*-butyl-substituted bipyridines should increase the ruthenium (4d) orbitals, thus increasing the energy gap with the occupied bridge orbitals. However this effect could not be reproduced at the extended Hückel level: the energies of the Ru(4d) orbitals were found insensitive to the substitution by *tert*-butyl groups on ancillary pyridines, probably because this non-SCF method cannot describe correctly the effects of charge displacements.

Conclusions

The [Ru(bpy)₂(ppX)] fragment has proved a useful starting point for the rational construction of models of molecular wires,

(26) Taking into account the very low energy barrier for rotation around a triple bond, ca. 0.5 kcal/mol (Levitus, M.; Schmieder, K.; Ricks, H.; Shimizu, K. D.; Bunz, U. H. F.; Garcia-Garibay, M. A. *J. Am. Chem. Soc.* **2001**, *123*, 4259–4265), the correct procedure would be to determine the potential energy versus angle profile, then compute the V_{ab} coupling as a function of the torsion angle, and finally compute a Boltzmann-averaged value. This is clearly outside the scope of this work, and for comparison purposes, the geometry was fixed planar.

(27) Taylor, P. N.; Wylie, A. P.; Huuskonen, J.; Anderson, H. L. *Angew. Chem., Int. Ed.* **1998**, *37*, 986. Piet, J. J.; Taylor, P. N.; Anderson, H. L.; Osuka, A.; Warman, J. M. *J. Am. Chem. Soc.* **2000**, *122*, 1749–1757.

(28) Nelsen, S. F.; Ismagilov, R. F.; Powell, D. R. *J. Am. Chem. Soc.* **1998**, *120*, 1924–1925.

(29) Sutter, J.-P.; Grove, D. M.; Beley, M.; Collin, J.-P.; Veldman, N.; Spek, A. L.; Sauvage, J.-P.; Van Koten, G. *Angew. Chem., Int. Ed. Engl.* **1994**, *33*, 1282–1284.

(30) Karafiloglou, P.; Launay, J.-P. *Chem. Phys.* **2003**, *289*, 231–242.

using a modular strategy with a systematic application of the Sonogashira coupling. A large variety of spacers can be employed to link the ruthenium moieties, thus allowing a detailed investigation of their efficiency to mediate intramolecular electron transfer. The detailed comparison of V_{ab} values as a function of metal–metal distances shows that the present series is one of the best, i.e., it gives among the largest couplings for a given length,^{1f,g} with a particularly high value in the case of the anthracene-containing bridge. All these results can be reproduced and rationalized by simple calculations, at the extended Hückel level. As a consequence, electron transfer can be monitored over distances approaching 20 Å, which is large enough to allow the insertion of an active moiety. Thus we have shown elsewhere that the association of the present redox units with a photochromic spacer allows the demonstration of molecular switching, by turning ON and OFF an intervalence transition.²¹

Experimental Part

General Instrumentation and Materials. NMR spectra were recorded on a Bruker 250 MHz, using the residual nondeuterated solvent as reference. For the complexes, reproducible data were obtained using a maximum of 10 mg of sample per tube in 0.5 mL of CD₃CN with, if needed, the addition of one drop of a diluted hydrazine solution in the same solvent (1 drop of N₂H₄·H₂O in 0.5 mL of solvent) to destroy paramagnetic impurities. FIDs were analyzed using MestRe-C 1.5.1³¹ or Swan-MR346³² programs. Mass spectra were recorded by the Service de Spectrométrie de Masse of the Université Paul Sabatier, using FAB (Nermag R10-R10, NBA matrix) or ES (Perkin-Elmer Sciex System API 100 or API 365).

Reagents and anhydrous DMF were all commercially available and were used as received; other anhydrous solvents were distilled from the appropriate drying agent (THF from sodium/benzophenone, amines from potassium hydroxide, and dichloromethane from calcium hydride). 9,10-Diiodoanthracene,³³ 9,10-bis(trimethylsilyl)ethynylanthracene,¹¹ 2,5-bis(trimethylsilyl)ethynylthiophene, 1,4-bis(trimethylsilyl)ethynylbenzene (adapted from ref 11), 9,10-bis[(2'-hydroxyprop-2'-yl)ethynyl]anthracene,¹³ 2-iodo-5-trimethylsilylthiophene,²² complexes **1-Br**, **1-I**, **12** (butynol),^{8,34} and terminal alkyne **13**²¹ were prepared following literature procedures. All experiments were carried out under an argon atmosphere using standard Schlenk tube techniques except where otherwise mentioned.

General Procedure for Dinuclear Complexes 2–4 and 2* and 3*. A solution of complex **1-Br** (150 mg, 0.19 mmol), Pd(PPh₃)₄ (10 mg, 0.01 mmol), CuI (10 mg, 0.05 mmol), and 0.09 mmol of the bis(trimethylsilyl)ethynylarene in 2 mL of DMF was heated under argon for 15 h with 1 pellet of NaOH (0.1 g, 2.5 mmol) (the reaction was followed by TLC on silica gel (MeCN/toluene, 1:1)), then the solvent was removed in vacuo. To the red residue was added NH₄PF₆ (100 mg) followed by acetonitrile (5 mL). The solution was stirred, then evaporated to dryness. The solid was then retaken in CH₂Cl₂, in which the excess of PF₆ salt is not soluble and deposited on a preparative TLC plate. After elution (toluene/MeCN, 6:4) the complex was desorbed from the silica by soaking it in a concentrated NH₄PF₆ solution in MeCN. After removal of the solvent, the residue was retaken in CH₂Cl₂, then the solution was concentrated and diethyl ether was added to precipitate the complex.

Complex 2. Yield: 51 mg (34%). ¹H NMR [CD₃CN] δ vs TMS: 6.65 (d, *J* = 7.8, 2H), 7.02 (td, *J* = 6.5, 1.4, 1H), 7.31–7.29 (m, 8H),

7.44 (td, *J* = 6.5, 1.2, 2H), 7.64 (dd, *J* = 5.6, 0.8, 2H), 7.71 (dd, *J* = 6.8, 3.3, 4H), 7.74–7.91 (m, 8H), 8.01 (td, *J* = 7.9, 1.7, 2H), 8.1 (dd, *J* = 5.6, 0.8, 2H), 8.25 (d, *J* = 8.0, 2H), 8.30 (d, *J* = 1.5, 2H), 8.33–8.43 (m, 6H), 8.48 (d, *J* = 8.2, 2H), 8.76 (dd, *J* = 6.7, 3.3, 4H). IR (KBr) $\nu_{C=C}$: 2093 cm⁻¹. FAB-MS (NBA matrix) *m/z*: 1503 [M – PF₆ + H]⁺, 679 [M – 2PF₆]²⁺.

Complex 3. Yield: 58 mg (39%). ¹H NMR [CD₃CN] δ vs TMS: 6.54 (d, *J* = 8.0, 2H), 6.92–7.01 (m, 4H), 7.15 (s, 2H), 7.17–7.27 (m, 6H), 7.43 (ddd, *J* = 7.5, 5.4, 1.1, 2H), 7.60 (dd, *J* = nr, 2H), 7.70–7.89, (m, 14H), 7.97–8.04 (m, 6H), 8.08 (d, *J* = 8.3, 2H) 8.32–8.35 (m, 4H), 8.39 (d, *J* = 7.9, 2H), 8.47 (d, *J* = 8.3, 2H). IR (KBr) $\nu_{C=C}$: 2193 cm⁻¹. ES-MS *m/z*: 1409 [M – PF₆]⁺, 851 [M – 2PF₆ – (Ru(bpy)₂)]⁺, 632 [M – 2PF₆]²⁺.

Complex 4. Yield: 88 mg (60%). ¹H NMR [CD₃CN], δ vs TMS: 6.54 (d, *J* = 7.8, 2H), 6.95–7.02 (m, 4H), 7.43 (td, *J* = 6.1, 1.1, 2H), 7.48 (s, 4H), 7.61 (dd, *J* = 5.6, 1.1, 2H), 7.70–7.89 (m, 14H), 7.97–8.05 (m, 6H), 8.09 (d, *J* = 7.9, 2H), 8.32–8.36 (m, 4H) 8.40 (d, *J* = 7.8, 2H) 8.47 (d, *J* = 8.1, 2H). IR (KBr) $\nu_{C=C}$: 2200 cm⁻¹. ES-MS *m/z*: 1403 [M – PF₆]⁺, 845 [M – 2PF₆ – (Ru(bpy)₂)]⁺, 628 [M – 2PF₆]²⁺.

Complex 2*. 9,10-Bis(trimethylsilyl)anthracene (18 mg, 0.05 mmol) was reacted with complex **1-Br*** (0.1 g, 0.1 mmol) with identical amounts of catalyst, NaOH, and DMF as for **2–4**. Preparative TLC was eluted first with pure CH₂Cl₂ then with CH₂Cl₂/MeOH, 9.5:0.5. Yield: 20 mg (20%). ¹H NMR [CD₃CN] δ vs TMS: 1.36 (s, 18H), 1.38 (s, 18H), 1.39 (s, 18H), 1.42 (s, 18H), 6.67 (d, *J* = 7.7, 2H), 7.05 (t, *J* = 7.02, 2H), 7.25–7.34 (m, 8H), 7.49 (dd, *J* = 6.0, 1.8, 2H), 7.60–7.79 (m, 14H), 7.98 (d, *J* = 6.4, 2H), 8.26 (d, *J* = 8.0, 2H), 8.30–8.5 (m, 10H), 8.73–8.78 (m, 4H). IR (KBr) $\nu_{C=C}$: 2094 cm⁻¹. ES-MS *m/z*: 1953 [M – PF₆]⁺, 904 [M – 2PF₆]²⁺.

Complex 3*. It was prepared on the same scale as for **2***, using the same protocol. Yield: 26 mg (25%). ¹H NMR [CD₃CN] δ vs TMS: 1.36 (s, 18H), 1.38 (s, 18H), 1.39 (s, 18H), 1.42 (s, 18H), 6.56 (d, *J* = 7.2, 2H), 6.91 (dd, *J* = 7.7, 1.3, 2H), 6.99 (t, *J* = 6.1, 2H), 7.13 (s, 2H), 7.20–7.29 (m, 6H), 7.46 (dd, *J* = 5.8, 1.7, 2H), 7.55–7.63 (m, 6H), 7.69–7.74 (m, 4H), 7.86 (d, *J* = 6.1, 2H), 7.96 (d, *J* = 1.3, 2H), 8.06 (d, *J* = 7.7, 2H), 8.33–8.35 (m, 4H), 8.38 (d, *J* = 1.8, 2H), 8.45 (d, *J* = 1.5, 2H). IR (KBr) $\nu_{C=C}$: 2194 cm⁻¹. ES-MS *m/z*: 856 [M – 2PF₆]²⁺.

Complex 5. A solution of complex **12** (70 mg, 0.09 mmol) and CuI (20 mg, 0.1 mmol) in DMF (4 mL) was heated in air with a KOH pellet for 15 h at 80 °C. The workup and preparative TLC were performed as for the other dinuclear complexes. Yield: 20 mg (30%). ¹H NMR [CD₃CN] δ vs TMS: 6.51 (d, *J* = 7.7, 2H), 6.94 (dd, *J* = 7.7, 1.8, 2H), 6.99 (td, *J* = 6.5, 1.4, 2H), 7.19–7.27 (m, 6H), 7.43 (td, *J* = 6.0, 1.1, 2H), 7.61 (d, *J* = 5.4, 2H), 7.70–7.88 (m, 14H), 7.97–8.05 (m, 6H), 8.07 (d, *J* = 8.0, 2H), 8.31–8.35 (m, 4H), 8.39 (d, *J* = 8.2, 2H), 8.46 (d, *J* = 8.1, 2H). IR (KBr) $\nu_{C=C}$: 2105 cm⁻¹. ES-MS *m/z*: 1326 [M – PF₆]⁺, 769 [M – 2PF₆ – (Ru(bpy)₂)]⁺, 591 [M – 2PF₆]²⁺.

Complex 7. To a well-degassed solution of complex **1-I** (42 mg, 0.05 mmol) and alkyne **13** (0.05 mmol) in DMF (1.5 mL) were successively added Pd(PPh₃)₄ (10 mg, 0.01 mmol), CuI (10 mg, 0.05 mmol), and 1.5 mL of diisopropylamine. The mixture was stirred at room temperature for 15 h. The complex was purified as usual. Yield: 30 mg (40%). ¹H NMR [CD₃CN] δ vs TMS: 6.49 (d, *J* = 7.8, 2H), 6.92 (dd, *J* = 7.6, 1.6, 2H), 6.97 (td, *J* = 6.6, 1.4, 2H), 7.19–7.26 (m, 6H), 7.42 (td, *J* = 6.5, 1.1, 2H), 7.50–8.09 (m, 24H), 8.31–8.36 (m, 4H), 8.39 (d, *J* = 8.0, 2H), 8.47 (d, *J* = 8.0, 2H). ES-MS *m/z*: 745 [M – 2PF₆ – (Ru(bpy)₂)]⁺.

Complex 15. To a well-degassed solution of 2-iodo-5-trimethylsilylthiophene (55 mg, 0.18 mmol) and alkyne **13** (0.18 mmol) in DMF (1.5 mL) were successively added Pd(PPh₃)₄ (10 mg, 0.01 mmol), CuI (10 mg, 0.05 mmol), and 2 mL of diisopropylamine. The mixture was stirred at room temperature for 6 h. After a usual ion-exchange procedure, the complex was purified by column chromatography (SiO₂,

(31) MestRe C 1.5.1, a freeware program for NMR data processing. Cobas, J. C.; Cruces, J.; Sardina, F. J. <http://qobruce.usc.es/jsrgroup/MestRe-C/MestRe-C.html>.

(32) Balacco, G. *J. Chem. Inf. Comput. Sci.* **1994**, *34*, 1235.

(33) Duerr, B. F.; Chung, Y.-S.; Czarnik, A. W. *J. Org. Chem.* **1988**, *53*, 2120–2122.

(34) Coudret, C.; Frayssé, S.; Minc, F.; Launay, J.-P. Manuscript in preparation.

CH_2Cl_2 , MeOH gradient 0 to 5%). Yield: 60 mg (65%). ^1H NMR [CD_3CN] δ vs TMS: 0.24 (s, 9H), 6.54 (d, $J = 7.7$, 1H), 6.90–7.01 (m, 2H), 2.10 (d, $J = 3.7$, 1H), 7.16 (d, $J = 4.0$, 1H), 7.17–7.27 (m, 3H), 7.42 (td, $J = 5.6$, 1.0, 1H), 7.61 (d, $J = 5.5$, 1H), 7.69–7.88 (m, 7H), 7.97–8.03 (m, 3H), 8.07 (d, $J = 7.9$, 1H), 8.31–8.35 (m, 2H), 8.38 (d, $J = 8.4$, 1H), 8.46 (d, $J = 8.3$, 1H). FAB-MS (NBA matrix) m/z : 770 [$\text{M} - \text{PF}_6$] $^+$.

Complex 6. To a well-degassed solution of complex **15** (60 mg, 0.07 mmol) in DMF (2 mL) was added a degassed solution of potassium hydroxide (0.5 mL, 6 M, 3 mmol), and the resulting mixture was heated for 10 min at 80 °C. After cooling, 9,10-diiodoanthracene (14.6 mg, 0.03 mmol), $\text{Pd}(\text{PPh}_3)_4$ (10 mg, 0.01 mmol), and CuI (10 mg, 0.05 mmol) were added and the resulting solution stirred for 8 h at room temperature. The workup and preparative TLC were performed as for the other dinuclear complexes. Yield: 18 mg (30%). ^1H NMR [CD_3CN] δ vs TMS: 6.56 (d, $J = 7.8$, 2H), 6.96–7.02 (m, 4H), 7.20–7.26 (m, 6H), 7.28 (d, $J = 3.8$, 2H), 7.43 (td, $J = 6.4$, 1, 2H), 7.55 (d, $J = 3.9$, 2H), 7.59–7.63 (m, 2H), 7.70–7.90 (m, 18H), 7.90–8.07 (m, 6H), 8.10 (d, $J = 7.8$, 2H), 8.33–8.44 (m, 6H), 8.47 (d, $J = 8.2$, 2H), 8.65 (dd, $J = 6.7$, 3.2, 4H). IR (KBr) $\nu_{\text{C}=\text{C}}$: 2190 cm^{-1} . ES-MS m/z : 1715 [$\text{M} - \text{PF}_6$] $^+$, 1157 [$\text{M} - 2\text{PF}_6 - (\text{Ru}(\text{bpy})_2)$] $^+$, 785 [$\text{M} - 2\text{PF}_6$] $^{2+}$.

Physicochemical Measurements and Computations. (a) Electrochemistry. Cyclic voltammetry was performed with a PC-controlled AUTOLAB PGSTAT20 potentiostat using the GPES 4.4 software. The working electrode was a 1 mm platinum button, and the reference electrode an aqueous saturated calomel electrode with a double frit system. The solvent was DNA-synthesis grade acetonitrile containing 0.1 M tetrabutylammonium hexafluorophosphate. For differential pulse voltammetry, a Metrohm rotating electrode with a Pt end was used, with rotation rate 1000 rpm and pulses of 25 mV amplitude and 70 ms duration.

(b) Spectroelectrochemistry and Determination of Metal–Metal Couplings. Intervalence transitions were recorded during controlled potential electrolysis in a special two-compartment electrolysis cell

described elsewhere.³⁵ The working electrode was a platinum grid. The advancement of the electrolysis was followed coulometrically and by voltammetry on the rotating electrode. At given intervals, the electrolysis was stopped, and the solution was transferred in 0.2 cm cells for measurements and then transferred back in the electrolysis cell. UV–vis–near-IR spectra were collected on a Shimadzu UV-PC 3101 spectrophotometer.

(c) Molecular Modeling and Quantum Chemical Calculations. Molecular geometry was optimized using the Cerius2 package.³⁶ The force field was Universal³⁷ with Ru–N and Ru–C bonds defined by $K_b = 350 \text{ kcal mol}^{-1} \text{ \AA}^{-2}$ and $R_0 = 2.05 \text{ \AA}$ (N) or 2.02 \AA (C). The geometry was fixed planar for aromatic cycles connected by triple bonds, and in order to facilitate the orbital analysis, a definite symmetry was imposed; that is, the dimer molecules were built with an inversion center (or a mirror symmetry in the case of **3**), corresponding to a $\Delta\Lambda$ configuration. For complexes **2*** and **3***, the *tert*-butyl groups were replaced by methyl groups to save computation time. Then extended Hückel calculations were performed in the Hyperchem³⁸ environment, using default parameters except for the H_{ii} energy of Ru(4d) orbitals taken as -11.5 eV as explained above. Electronic coupling values (V_{ab}) were obtained by the “dimer splitting” method as described elsewhere.^{4b}

Acknowledgment. The author thank Mrs. Christine Viala for her technical assistance.

Supporting Information Available: This material is available free of charge via the Internet at <http://pubs.acs.org>.

JA0299506

(35) Patoux, C.; Coudret, C.; Launay, J.-P.; Joachim, C.; Gourdon, A. *Inorg. Chem.* **1997**, *36*, 5037.

(36) Cerius2; Accelrys Inc.: San Diego, CA; 2001.

(37) Universal Force Field; Rappe, A. K.; Casewit, C. J.; Colwell, K. S.; Goddard, W. A., III; Skiff, W. M. *J. Am. Chem. Soc.* **1992**, *114*, 10024.

(38) Hyperchem, version 6.01; Hypercube, Inc.: Gainesville, FL; 2000.